Formation of Chromium Nitride and Intragranular Austenite in a Super Duplex Stainless Steel

N. HOLLÄNDER PETTERSSON, D. LINDELL, F. LINDBERG, and A. BORGENSTAM

Precipitation of chromium nitrides and formation of intragranular austenite were studied in detail for the super duplex stainless steel grade 2507 (UNS S32750). The situation of multipass welding was simulated by heat treatment at 1623 K (1350 °C) and quenching followed by short heat treatments at 1173 K (900 °C). The microstructural evolution was characterized using transmission and scanning electron microscopy, electron backscatter, and transmission Kikuchi diffraction, and it was observed that the interior of the ferrite grains contained chromium nitrides after quenching. The nitrides were predominantly of CrN with a cubic halite-type structure and clusters of CrN-Cr_2N where rod-shaped trigonal Cr_2N particles had nucleated on plates of CrN. After heat treatment for 10 seconds at 1173 K (900 °C), the nitride morphology was transformed into predominantly rod-shaped Cr_2N, and finely dispersed intragranular secondary austenite idiomorphs had formed in the nitride-containing areas within the ferrite grains. After 60 seconds of heat treatment, both the Cr_2N nitrides and the secondary austenite were coarsened. Analysis of electron diffraction data revealed an inherited crystallographic relationship between the metastable CrN and the intragranular austenite. The mechanism of chromium nitride formation and its relation to secondary austenite formation in duplex stainless steels are discussed.

https://doi.org/10.1007/s11661-019-05489-2

I. INTRODUCTION

DUPLEX stainless steels, consisting of ferrite and austenite, possess a unique combination of high corrosion resistance in combination with high mechanical strength. The properties are influenced by the balance of the two constituent phases, and duplex stainless steels are generally solution heat treated to generate a fine-grained microstructure of 50 pct ferrite and 50 pct austenite. However, during welding, this fine-grained and balanced microstructure is degenerated, and a new microstructure is formed through a dynamic interplay between the ferrite and the austenite with change in temperature. At temperatures close to solidus, the duplex microstructure transforms into single-phase ferrite which rapidly coarsens.[1,2] During cooling, the austenite forms as Widmanstätten structure or grain boundary allotriomorphs, and the weldability is significantly improved by alloying with nitrogen that acts as a strong austenite former and increases austenite transformation kinetics.[3–5] Too slow cooling can promote precipitation of intermetallic phases (χ and σ) and Cr_2N in grain or phase boundaries in the critical temperature range 1273 K down to 973 K.[6–9] A rapid cooling (or quenching), on the other hand, will generate a high density of chromium nitrides in the interior of the ferrite grains as a result of supersaturation with respect to nitrogen.[10–14] In multipass welding, this microstructure of supersaturated ferrite grains, potentially with chromium nitrides, in the heat-affected zone (HAZ) becomes repetitively heat treated due to heat transfer from subsequent passes. It is not only important to understand the precipitation that occurs during quenching but also the transformations during an additional heat treatment to control the properties.

It has been reported that in addition to trigonal Cr_2N, also CrN with a cubic halite-type structure is formed upon rapid quenching of duplex stainless steels.[3,11–13] CrN is often seen as plates surrounding the Cr_2N particles; however, the reason to this is not yet fully understood. It is further known that a second heat treatment promotes the formation of secondary austenite (designated γ_2) that grows on the preexisting

N. HOLLÄNDER PETTERSSON is with the Swerim AB, Isafjordsgatan 28A, 164 40 Stockholm, Sweden and also with the Department of Materials Science, KTH Royal Institute of Technology, Brinellvägen 23, 114 28 Stockholm, Sweden. Contact e-mail: nikpet@kth.se D. LINDELL and F. LINDBERG are with the Swerim AB. A. BORGENSTAM is with the Department of Materials Science, KTH Royal Institute of Technology.

Manuscript submitted May 17, 2019.
Article published online October 11, 2019

austenite grains,[15,16] or by formation of intragranular idiomorphs in the ferrite.[15,17] Ramirez *et al.*[15,18] suggested that the formation of intragranular austenite could be related to chromium nitrides; however, this mechanism was never confirmed. This is important to understand since the nitrides and intragranular austenite are prone to form in duplex stainless steel welds, and in particular, the intragranular austenite can lead to a decreased corrosion resistance.[19]

The purpose of the current study has been to study the chromium nitride precipitation and its relation to intragranular γ_2 for a super duplex stainless steel. The nitride precipitation and secondary austenite formation mechanisms are finally discussed.

II. EXPERIMENTAL DETAILS

A. *Material and Heat Treatments*

Plate material of super duplex grade 2507 (UNS S32750) with a thickness of 6 mm was delivered by Outokumpu Stainless AB. The chemical composition from the plate certificate is given in Table I. Cylindrical specimens of Ø4 × 8 mm was machined out from the 6 mm plate. The heat treatments were performed in a Bähr 805 A/D dilatometer in protective helium atmosphere, and the temperature was controlled by a thermocouple soldered to the surface of the specimen. Figure 1 shows the programmed and measured temperature cycles. The specimens were initially heated to 1623 K (1350 °C) at 100 K/s, held for 3 seconds, and then quenched to room temperature at 300 K/s. The purpose of the initial heat treatment was to resemble the temperature exposure in HAZ, and the high cooling rate was applied to produce high nitrogen supersaturation within ferrite and thus a high driving force for nitride formation. After quenching to ambient temperature, the specimens were subjected to a subsequent heat treatment at 1173 K (900 °C) for 10 and 60 seconds (the heating and cooling rate was 100 K/s) to study the influence of subsequent heat treatment on the HAZ-simulated and quenched microstructure.

B. *Electron Microscopy*

The microstructures were investigated by scanning electron microscopy (SEM) and electron backscattered diffraction (EBSD). Preparation of cross sections for SEM was done by standard metallographic methods and final polishing in a colloidal silica solution (with 40 nm sized particles) using a vibratory polisher. The SEM analysis was performed using a JEOL 7001F field-emission gun (FEG) microscope equipped with the NordlysNano EBSD detector from Oxford Instruments. The acquisition software used was AZtec 3.1, and postprocessing was performed using the HKL CHANNEL5 software package. The EBSD analysis was performed using a 10 kV acceleration voltage.

The fine-scaled nitride morphology in the quenched sample was investigated by transmission electron microscopy (TEM) in a JEOL 2100F FEG microscope operated at 200 kV. Thin foils were prepared by electrolytic polishing using a twin-jet polisher at 12 V in an electrolyte of 15 pct perchloric acid in methanol kept at 255 K (− 18 °C). The thin foils were cleaned by argon ion polishing in a Gatan precision ion-polishing system prior to analysis. The nitrides were further analyzed by orientation mapping through transmission Kikuchi diffraction (TKD) performed on carbon extraction replica samples. The carbon extraction replicas were prepared by coating cross sections with a 10-nm layer of carbon using a Gatan precision etching and coating system. The carbon layer was etched free from the specimen surface using a solution of 100 mL HCl, 20 mL HNO_3, and 100 mL H_2O heated to 323 K (50 °C). Etched-free pieces of carbon were washed in ethanol, stretched in distilled H_2O, and transferred to copper grids. The TKD analysis was performed using a 30 kV acceleration voltage and a 10-nm step size.

Orientation relationships (ORs) between ferrite, CrN, Cr_2N, and austenite were studied by comparing calculated orientations *via* different idealized ORs with experimental orientation data using the MTEX toolbox for Matlab.[20]

III. RESULTS AND DISCUSSION

A. *The As-quenched Microstructure and Nitride Morphology*

After the initial heat treatment and quenching (300 K/s from 1623 K (1350 °C)), the microstructure (see Figure 2) consisted of mainly equiaxed ferrite grains and austenite in the form of Widmanstätten and grain boundary allotriomorphs, and as expected, areas are also seen where the original austenite morphology is preserved. The austenite is not expected to fully dissolve in this alloy until 1648 K (1375 °C),[2] and the amount of undissolved austenite appeared similar throughout the sample. Virtually all ferrite grains contained nitrides, the precipitates are concentrated in the center of the grains, and both plate-like and rod-shaped morphologies are observed (see Figures 3(a) and (b)). In higher resolution using STEM, a mixed nitride morphology is distinguished (see Figures 4(a) and (b)), and a fine dispersion of nanosized precipitates are seen within the ferrite (see Figure 4(c)). It has previously been reported that CrN can precipitate during cooling of duplex stainless steels and is often found mixed with the Cr_2N. In agreement with the present case, the CrN has been reported to have a disk-like or plate-like morphology, while the Cr_2N appears as rod-shaped particles adjacent to the CrN phase.[11–13] The crystal structures of these different nitride precipitates were identified by selected area electron diffraction as cubic halite-type CrN ($Fm\bar{3}m$) and trigonal Cr_2N ($P\bar{3}1m$) in a previous study.[13]

When observing the morphologies, it appears that CrN has precipitated from ferrite, while the Cr_2N seems related to the CrN. The crystallographic OR of CrN relative to the parent ferrite grain was identified from

Table I. The Chemical Composition (in Weight Percent) of the Duplex Grade 2507 (UNS S32750) Measured Using Combined X-ray Fluorescence and Combustion Analysis (The Batch Analysis)

C	Si	Mn	P	S	Cr	Ni	Mo	N	Cu
0.12	0.30	0.83	0.023	0.001	24.84	6.90	3.80	0.28	0.18

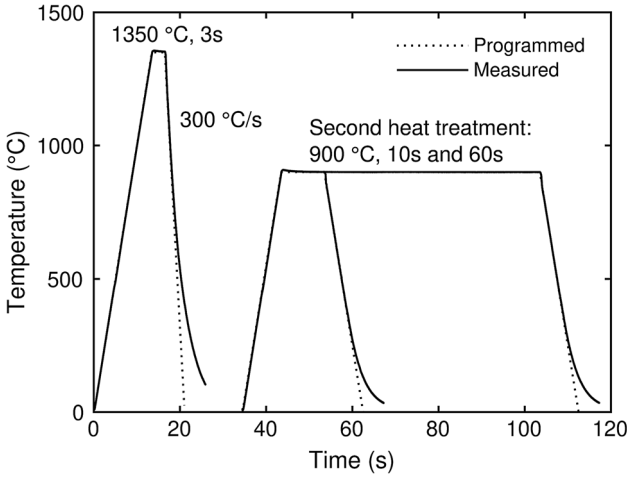

Fig. 1—Time–temperature profile showing the three heat treatments performed in dilatometer: 1623 K (1350 °C) for 3 s and quenched 300 K/s followed by subsequent heat treatments at 1173 K (900 °C) for 10 and 60 s.

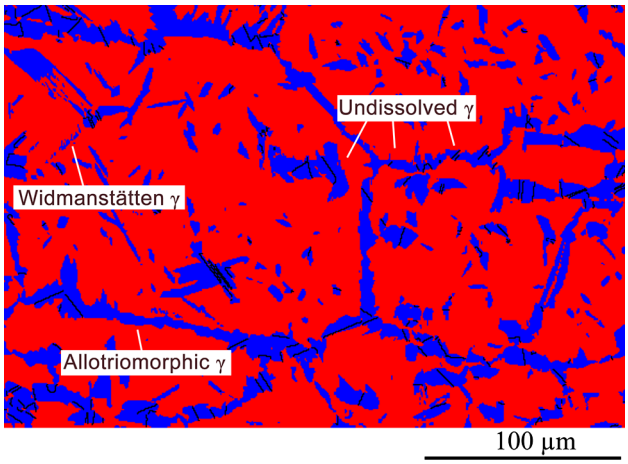

Fig. 2—A phase-colored EBSD map showing an overview of the quenched microstructure (ferrite colored in red and austenite in blue) consisting of coarse ferrite grains and different morphologies of austenite. Note that the nitrides are not detected in this map due to their small size (Color figure online).

pole figures constructed from EBSD data (the details are not presented here) as the Baker–Nutting OR $(100)_{\alpha}||(100)_{CrN}$ and $[110]_{\alpha}||[100]_{CrN}$. This is the same OR found for CrN precipitates in nitrided ferritic chromium steels.[21,22] It should be noted that this OR was not holding good for all CrN. One reason for this could be that preferential nucleation at ferrite subboundaries could result in an irrational OR compared to nucleation within the ferrite lattice.

The integrated morphology of CrN and Cr_2N was further investigated by orientation mapping on extraction replicas using TKD (see Figure 5). In the phase-colored map, the rods are identified as Cr_2N (blue), while the plates/disks are mainly indexed as CrN (red). In addition to rods, Cr_2N with a cluster-like morphology is also identified which will be discussed further based on crystallographic analyses.

B. *Microstructure Evolution Upon Reheating at 1173 K*

The quenched nitride-containing microstructure was subjected to additional short heat treatments to simulate the multipass welding situation. After reheating at 1173 K (900 °C), the most apparent changes occurred within the ferrite grains. Overviews of the ferrite grain interiors after 10 and 60 seconds of reheating are shown in Figures 3(c) through (f), respectively. From microstructural observations, three main processes are identified to have been initiated during the heat treatment for 10 seconds (see Figures 3(c) and (d)).

- In all nitride-containing ferrite grains, CrN has disappeared and the nitride morphology only consists of rod-shaped Cr_2N particles with a crystallographic OR to the ferrite matrix.
- Within many ferrite grains a high density of idiomorphic γ_2 has formed. The γ_2 are associated with nitrides, whereof some of the γ_2 also enclose nitrides. The network of γ_2 is more developed toward the center of the ferrite grains.
- The austenite has grown from the phase boundaries. This was concluded from the observation that the grain boundary allotriomorphs were coarser and were seen to enclose nitrides (see Figure 6) that were not observed in phase boundaries in the quenched condition. Precipitation of intergranular nitrides have been proposed to proceed growth of intergranular γ_2 at the existing austenite interface upon heat treatment.[15]

After 60 seconds of heat treatment at 1173 K (900 °C), most of the ferrite grains contained a network of γ_2 precipitates (see Figures 3(e) and (f)). The intragranular γ_2 was at this stage coarser and more evenly distributed within the ferrite grains. The Cr_2N had coarsened and were still distributed with the γ_2.

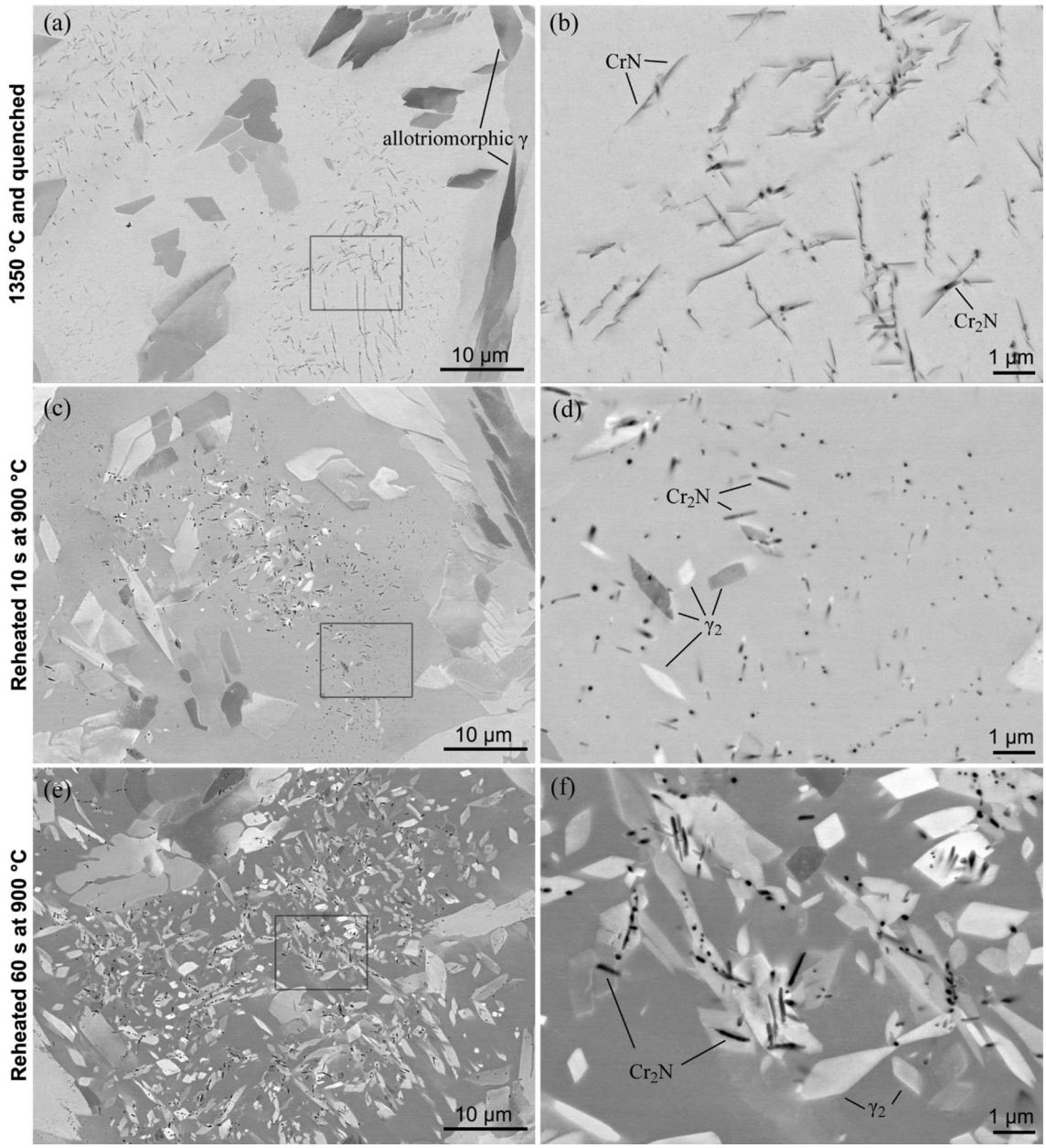

Fig. 3—Backscattered electron SEM images showing precipitates in the interior of the ferrite grain in (*a*) and (*b*) the quenched condition, and after additional heat treatment at 1173 K (900 °C) for 10 and 60 s in (*c*) and (*d*) and (*e*) and (*f*), respectively.

C. *Chromium Nitride Formation*

It appears that the clusters of CrN and Cr_2N represent an intermediate stage in the transition from a metastable state. After heat treatment at 1173 K (900 °C), CrN has transformed into rod-shaped Cr_2N that seems to be the preferred morphology and phase. Figure 7 shows a phase-colored EBSD map of the interior of a ferrite grain after 60 seconds at 1173 K (900 °C). The rod-shaped Cr_2N particles (green) are seen both in the ferrite matrix and within clusters of intragranular γ_2 (all austenite is colored blue), and sole Cr_2N particles that have adopted an apparent relation to the ferrite matrix are indicated. The Cr_2N (0001)-trace (the trace lines marked white), which is parallel to the rod-length, is always parallel to one $(110)_\alpha$-plane (the trace lines marked black). A comparison between the measured orientation of Cr_2N (in Figure 7) and the calculated orientation variants of the Cr_2N/ferrite OR $(110)_\alpha||(0001)_{Cr_2N}$ and $[\bar{1}11]_\alpha||[\bar{1}100]_{Cr_2N}$ [23] is shown in Figure 8(a). This OR holds for all Cr_2N particles in Figure 7 with one exception, namely particle marked with N_2 in the figure. However, as seen this particle is in an austenite subboundary. The association with this OR suggests that in clusters that enclose nitrides, see, *e.g.*, the γ_2 idiomorphs denoted A_1–A_3 and the nitride N_1 in Figure 7, the nitrides have existed prior to the γ_2.

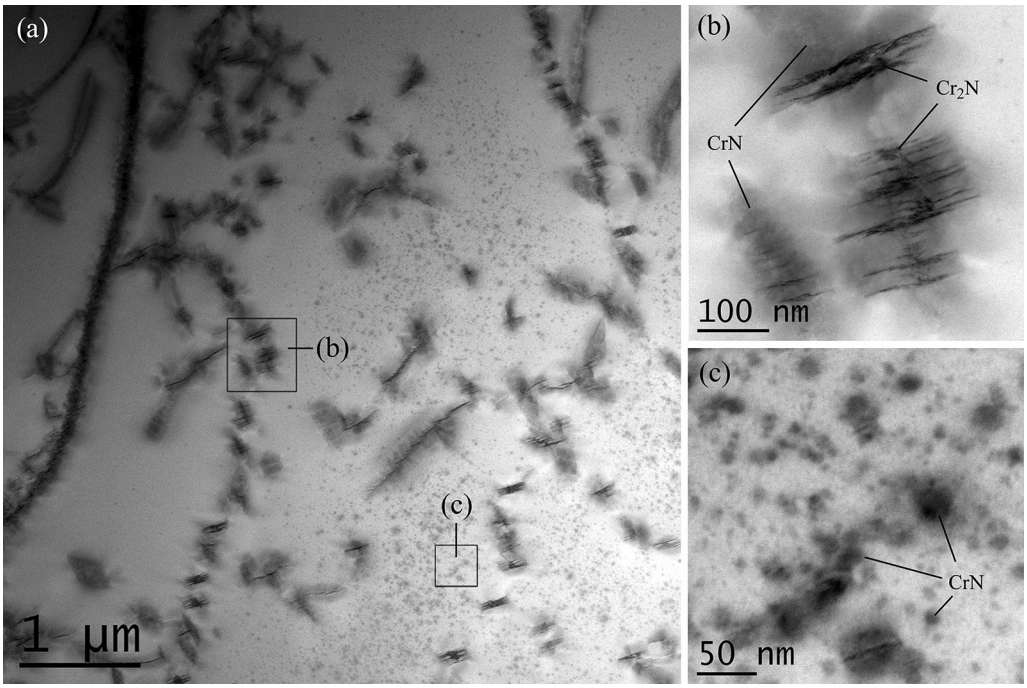

Fig. 4—STEM images from a thin foil specimen showing (*a*) overview of the different nitride morphologies after heat treatment 1623 K (1350 °C) and quenching with insets indicating (*b*) mixed CrN and Cr_2N, and (*c*) CrN.

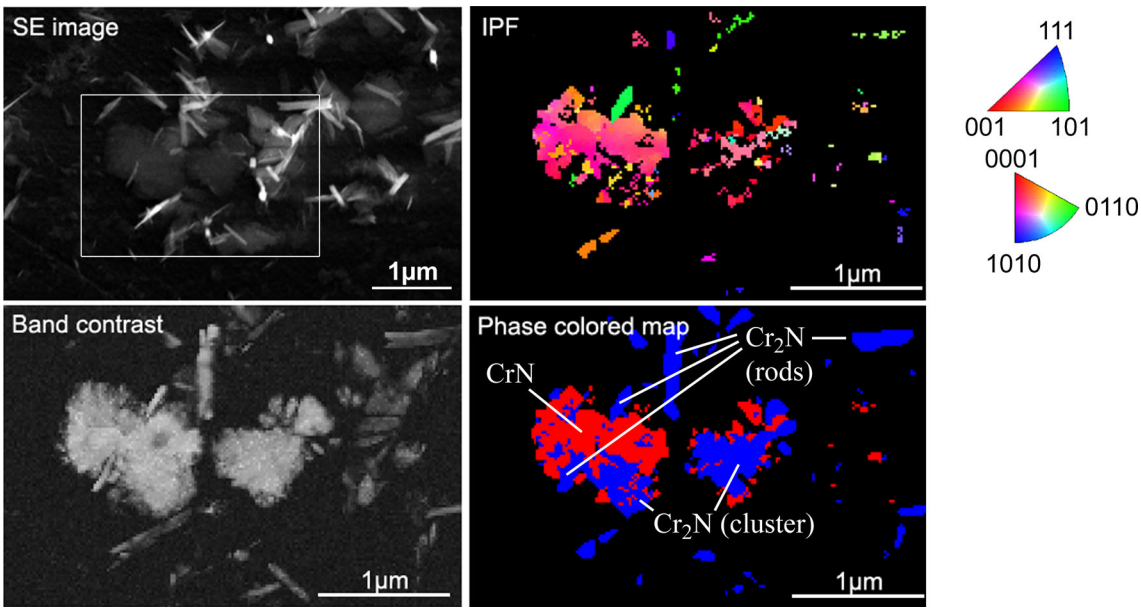

Fig. 5—A nitride colony consisting of CrN and Cr_2N in the quenched material analyzed using TKD (step size 10 nm) in the SEM from a carbon extraction replica in which the precipitates have been etched free from the bulk. Note that the Cr_2N is present both in rod-shaped and cluster-like morphologies (Color figure online).

The morphology of the CrN-Cr_2N clusters was further analyzed with respect to the orientations within individual clusters measured by TKD (see Figure 5). An OR was identified between CrN and Cr_2N matching the fcc-Cr_2N OR reported for high-nitrogen austenitic stainless steels,[24] in this case $(111)_{CrN}||(0001)_{Cr_2N}$ and $[\bar{1}10]_{CrN}||[\bar{1}100]_{Cr_2N}$ (see Figure 8(b)). This is reasonable due to the close resemblance of cubic halite-type crystal structure of CrN and the fcc structure of austenite. Transition of the nitride from austenite can be viewed as chromium enrichment and location of nitrogen to interstitial sites in the fcc lattice.

Rod-shaped and cluster-like morphology of Cr_2N were both present in the as-quenched state, whereas only the rod morphology is found after subsequent heat treatment at 1173 K (900 °C). In the following, a

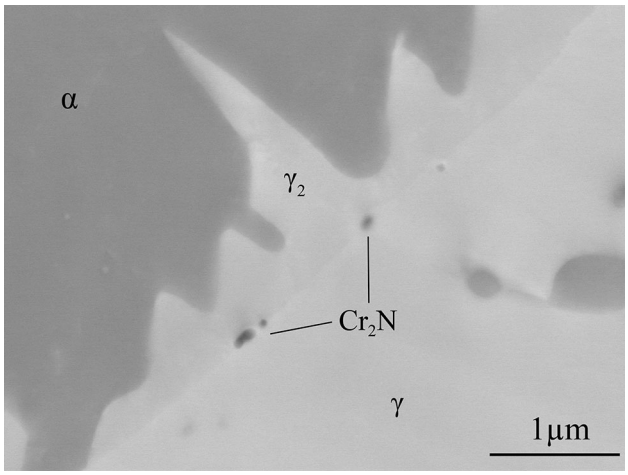

Fig. 6—Growth of austenite from the ferrite-austenite phase boundary after 10 s at 1173 K. Cr_2N has formed at the initial phase boundary followed by growth of γ_2.

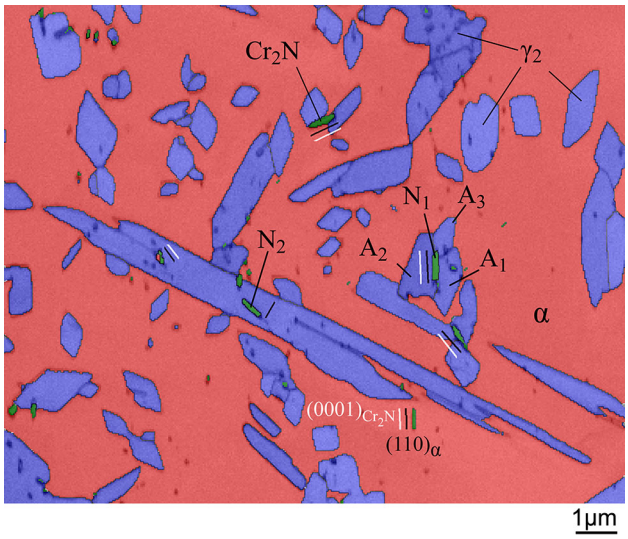

Fig. 7—Phase-colored map (step size 40 nm) of Cr_2N (green) and intragranular secondary austenite (blue) within the ferrite (red) after 60 s reheating at 1173 K (900 °C). Black lines show the trace of $(0001)_{Cr_2N}$, and white lines trace of the parallel $(110)_\alpha$ indicating the relation between the ferrite matrix and the particle shape. Note that for the nitride particle N_2, there is no such relation (Color figure online).

crystallographic assessment is made based on the TKD data from the extraction replica. The measured orientation of Cr_2N was compared to those calculated according to the identified CrN-Cr_2N and ferrite-Cr_2N ORs. Since the ferrite is not present in the replicas, its orientation had to be calculated based on the available Cr_2N. The ferrite orientation was established as the mean of the calculated orientations from particles in Figure 5). In Figure 8(c), the measured orientations of Cr_2N within a single CrN-Cr_2N cluster are compared to the calculated orientation variants according to the ORs with the CrN and the ferrite, respectively. The (0001) pole containing a single reflection for each particle is given for simplicity. It can be seen that the Cr_2N that has grown on CrN and developed a rod-shaped morphology is the variant that has a lower misorientation to the ferrite-Cr_2N OR.

It thus appears that CrN exists as a metastable initial stage in the nitride-precipitation process that nucleates Cr_2N during quenching. The CrN-Cr_2N clusters represent an intermediate stage leading to sole particles of Cr_2N as the CrN is dissolved and rod-shaped Cr_2N particles grows in the ferrite matrix during heat treatment at 1173 K (900 °C) in this case. The transformation from CrN to Cr_2N is presumably driven by local decrease of the nitrogen supersaturation in the ferrite due to formation of nitrides and growth of primary austenite since the CrN is expected to be stabilized by a high nitrogen activity.[25] Miyamoto *et al.*[26] reported the opposite situation, a transition in the nitride morphology due to nitrogen enrichments, for a Fe-18 mass pct Cr alloy plasma nitrided at 943 K (670 °C). In that case, CrN was observed in regions of high nitrogen activity, while only Cr_2N was found deeper into the nitrided zone where the nitrogen activity was lower. In an intermediate region, both CrN and Cr_2N existed where the CrN in that case had formed by transition from rod-shaped Cr_2N opposite to the present situation, in which the ferrite nitrogen level is decreasing.

D. *Intragranular Secondary Austenite Formation*

The nucleation of intragranular austenite is suppressed during quenching but precipitates in a high density during the second heat treatment; it seems to succeed the transformation of the CrN-Cr_2N clusters into sole particles of Cr_2N. To understand this better, the crystallographic relations have been investigated. The intragranular nucleated austenite has been reported to have a Kurdjumov–Sachs (K–S) OR,[27] $(011)_\alpha||(111)_\gamma$ and $[11\bar{1}]_\alpha||[10\bar{1}]_\gamma$, with the ferrite matrix,[10] and the here-measured orientation of γ_2 is rather close to the idealized K–S OR (see Figure 9(a)). The OR between the Cr_2N and γ_2 was further determined for individual γ_2 clusters, one example being the A_1–A_3 cluster in Figure 7. Each of the A_1–A_3 γ_2 particles holds an $(0001)_{Cr_2N}||(111)_\gamma$ and $[\bar{1}100]_{Cr_2N}||[\bar{1}10]_\gamma$ OR toward the adjacent Cr_2N particle N_1; noteworthy, this is the same type of OR identified between Cr_2N and CrN in the quenched microstructure. The measured orientation of A_1–A_3 compared to the calculated possible orientation variants based on the orientation of the nitride N_1 and of the ferrite matrix are shown in Figure 9(b). The A_1–A_3 γ_2 idiomorphs are oriented around one of the two pairing-variants of these ORs and are thus satisfying each OR at both the Cr_2N/γ_2 and the ferrite/γ_2 interfaces. Clusters were also found where some γ_2 did not fulfill the pairing-variant condition with the adjacent nitrides. There might be other nucleation events as will be further discussed, but one apparent reason is that γ_2 develops a dense network in which hard impingement inevitably occurs and it can be difficult in such cases to see a difference between nucleation and impingement.

A two-step nucleation mechanism has been proposed for the intragranular γ_2 in duplex stainless steels by Atamert and King,[28] Chen and Yang,[10] and Chen

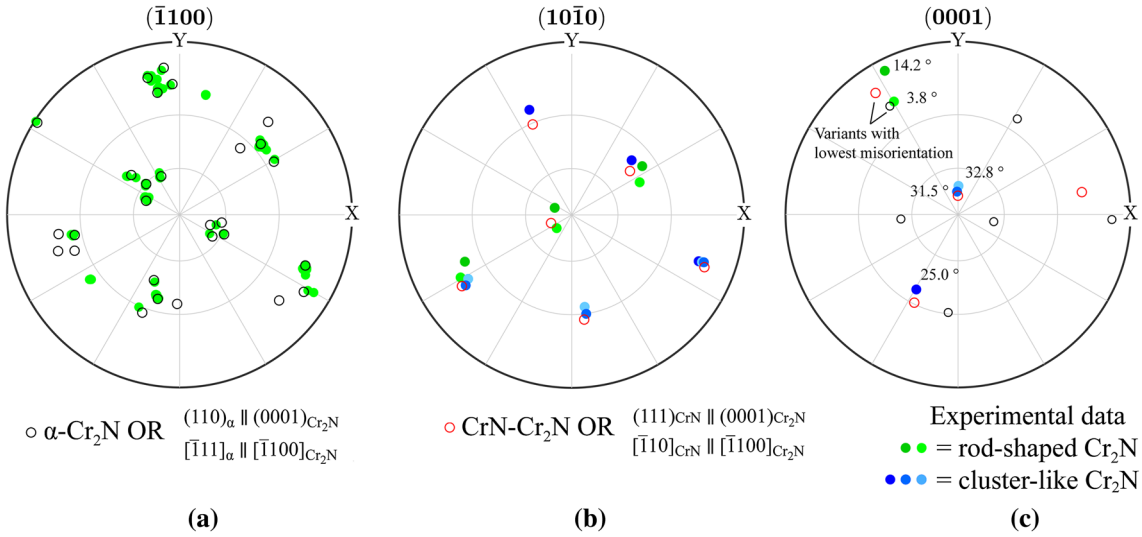

Fig. 8—Comparison of ideal OR (open circles) and experimental data (filled circles). (*a*) Calculated orientation variants of Cr_2N compared to the measured Cr_2N orientation after heat treatment 60 s at 1173 K (900 °C) (the data in Fig. 7); (*b*) calculated variants of Cr_2N in the nitride cluster (quenched condition) compared to measured ones including rod-shaped (green) and cluster-like (blue) Cr_2N morphologies (the data in Fig. 5); (*c*) the Cr_2N orientations in the nitride cluster compared to the OR adopted after heat treatment at 1173 K (900 °C) and the corresponding misorientations (Color figure online).

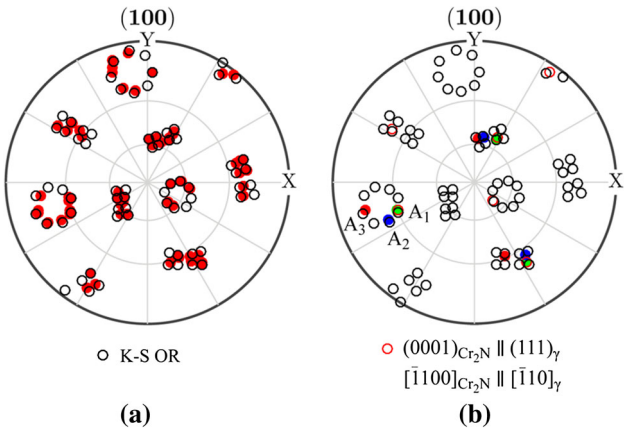

Fig. 9—Pole figures showing (*a*) measured orientation of intragranular austenite (filled symbols) compared to the K–S OR, and (*b*) pairing-variants of austenite in the K–S OR and the suggested Cr_2N/γ_2 OR (calculated from the orientation of the particle N_1) compared to orientation of three austenite particles denoted A_1–A_3 in Fig. 7 (filled symbol).

et al.[29] who pointed out that after the initial nucleation events, the idiomorphic γ_2 forms through sympathetic nucleation, *i.e.*, nucleation on faces or edges of preexisting austenite idiomorphs. Indications of this can be seen in Figure 7. However, the proposed mechanism requires an initiating nucleation event and the formation of γ_2 on nonmetallic inclusions have been suggested in several studies as a possible initial event.[10,15,28] However, this was not observed in the present case, and it would be surprising if the dense γ_2 networks within ferrite grains seen in Figures 3(e) and (f) are the result of a limited number of initial events. Ramirez *et al.*[18] discussed that nitrides could act as nucleation sites for γ_2 due to formation of low-energy interfaces between the $(0001)_{Cr_2N}$ and $(111)_{\gamma_2}$ planes. In fact, since Cr_2N has initially nucleated at metastable CrN with a similar OR, the rod-shaped Cr_2N is oriented such that the γ_2 forms low-energy interfaces toward both the ferrite by the K–S OR and to the Cr_2N. The formation of intragranular γ_2 is therefore presumably suppressed during quenching due to the lack of initial nucleation sites; however, upon the second heat treatment, high number of nucleation sites have developed with the Cr_2N. Considering the high density of Cr_2N found within the nitride-containing ferrite grains, this is probably a more governing mechanism in this case compared to the sympathetic nucleation.

IV. SUMMARY AND CONCLUSIONS

Chromium nitride precipitation and its relation to formation of intragranular austenite have been studied for the super duplex stainless steel 2507 using electron microscopy (SEM and TEM) and a combination of electron diffraction techniques (EBSD and TKD). The material was heat treated at 1623 K (1350 °C) and quenched and subjected to a second heat treatment at 1173 K (900 °C) to simulate the multipass weld situation.

The rapid quenching promoted nonequilibrium nitride formation in the supersaturated ferrite grain interiors. The nitrides were predominately of CrN halite-type structure, both nanosized intragranular precipitates, and in clusters with an integrated morphology of trigonal Cr_2N. In these clusters, a crystallographic OR was identified between the nitrides: $(111)_{CrN}||(0001)_{Cr_2N}$ and $[\bar{1}10]_{CrN}||[\bar{1}100]_{Cr_2N}$. The formation of CrN is likely an initial metastable stage in the chromium nitride-precipitation process, presumably favored by a lower activation energy that provides nucleation sites for, the in this case, more thermodynamically stable, Cr_2N.

Heat treatment for 10 seconds at 1173 K (900 °C) promoted a transformation of CrN-Cr_2N clusters into rods of Cr_2N, and intragranular idiomorphic γ_2 started forming. The Cr_2N particles that grew into rods have a well-defined OR to the ferrite: $(110)_\alpha||(0001)_{Cr_2N}$ and $[\bar{1}11]_\alpha||[\bar{1}100]_{Cr_2N}$ and represent the Cr_2N variants from CrN that better matches the preferred growth direction in the ferrite.

After 60 seconds at 1173 K (900 °C), the γ_2 and the Cr_2N had coarsened. The γ_2 were in several cases observed as clusters around Cr_2N particles with a $(0001)_{Cr_2N}||(111)_\gamma$ and $[\bar{1}100]_{Cr_2N}||[\bar{1}10]_\gamma$ OR while growing with a K–S OR toward the ferrite, suggesting that the nitrides are preferential nucleation sites. In fact, the γ_2 inherits the same crystallographic orientation to Cr_2N as formed *via* nucleation of Cr_2N from initial CrN during quenching.

The current study clearly shows that if chromium nitrides are present within the ferrite, there is an increased potential for formation of γ_2 if the quenched material is subjected to cyclic heat treatments, for example, as in case of multipass welding.

ACKNOWLEDGMENTS

Open access funding provided by Royal Institute of Technology. This study was performed within the Project Avon supported by Vinnova the Swedish Government Agency for Innovation Systems (Grant Number 2014-01874), and the Project Partners Outokumpu Stainless, Sandvik Materials Technology, NOMAC Norwegian Material Center of Expertise, KTH Royal Institute of Technology and Jernkontoret. Hugo Carlssons Stiftelse, Axel Hultgrens Stiftelse, and Gerhard Von Hofstens Stiftelse are also gratefully thanked for their support. Staffan Hertzman (Swerim) is thanked for comments on the manuscript.

OPEN ACCESS

REFERENCES

1. T.A. Palmer, J.W. Elmer, and S.S. Babu: *Mater. Sci. Eng. A*, 2004, vol. 374, pp. 307–21.
2. N. Pettersson, S. Wessman, S. Hertzman, and A. Studer: *Metall. Mater. Trans. A*, 2017, vol. 48A, pp. 1562–71.
3. S. Hertzman, W. Roberts, and M. Lindenmo: in *Proc. Conf. Duplex Stainless Steels'86,* Hague, The Netherlands, 1986, pp. 257–67.
4. S. Hertzman, B. Brolund, and P.J. Ferreira: *Metall. Mater. Trans. A*, 1997, vol. 28A, pp. 277–85.
5. S. Hertzman: *ISIJ Int.*, 2001, vol. 41, pp. 580–89.
6. J.-O. Nilsson: *Mater. Sci. Technol.*, 1992, vol. 8, pp. 685–700.
7. E. Bettini, U. Kivisäkk, C. Leygraf, and J. Pan: *Electrochim. Acta*, 2013, vol. 113, pp. 280–89.
8. N. Sathirachinda, R. Pettersson, S. Wessman, U. Kivisäkk, and J. Pan: *Electrochim. Acta*, 2011, vol. 56, pp. 1792–98.
9. D.C. Dos Santos and R. Magnabosco: *Metall. Mater. Trans. A*, 2016, vol. 47A, pp. 1–12.
10. T.H. Chen and J.R. Yang: *Mater. Sci. Eng. A*, 2002, vol. 338, pp. 166–81.
11. J. Liao: *ISIJ Int.*, 2001, vol. 41, pp. 460–67.
12. R.F.A. Jargelius-Pettersson, S. Hertzman, P. Szakalos, and P.J. Ferreira: in *Proc. Conf. Duplex Stainless Steels'94*, Glasgow, Scotland, 1994, pp. 461–72.
13. N. Pettersson, R.F.A. Pettersson, and S. Wessman: *Metall. Mater. Trans. A*, 2015, vol. 46A, pp. 1062–72.
14. E. Bettini and U. Kivisäkk: *Int. J. Electrochem. Sci.*, 2014, vol. 9, pp. 61–80.
15. A.J. Ramirez, J.C. Lippold, and S.D. Brandi: *Metall. Mater. Trans. A*, 2003, vol. 34A, pp. 1575–97.
16. C.M. Garzón and A.J. Ramirez: *Acta Mater.*, 2006, vol. 54, pp. 3321–31.
17. J.-O. Nilsson, L. Karlsson, and J.-O. Andersson: *Mater. Sci. Technol.*, 1995, vol. 11, pp. 276–83.
18. A.J. Ramirez, S.D. Brandi, and J.C. Lippold: *Sci. Technol. Weld. Join.*, 2004, vol. 9, pp. 301–13.
19. J.-O. Nilsson, T. Huhtala, P. Jonsson, L. Karlsson, and A. Wilson: *Metall. Mater. Trans. A*, 1996, vol. 27A, pp. 2196–2208.
20. F. Bachmann, R. Hielscher, and H. Schaeben: *Solid State Phenom.*, 2010, vol. 160, pp. 63–68.
21. B. Mortimer, P. Grieveson, and K.H. Jack: *Scand. J. Metall.*, 1972, vol. 1, pp. 203–09.
22. M. Sennour, P.H. Jouneau, and C. Esnouf: *J. Mater. Sci.*, 2004, vol. 39, pp. 4521–31.
23. K.A. Bywater and D.J. Dyson: *Met. Sci. J.*, 1975, vol. 9, pp. 155–62.
24. T.H. Lee, H.Y. Ha, B. Hwang, and S.J. Kim: *Metall. Mater. Trans. A*, 2012, vol. 43A, pp. 822–32.
25. S. Hertzman and M. Jarl: *Metall. Mater. Trans. A*, 1987, vol. 18A, pp. 1745–52.
26. G. Miyamoto, A. Yonemoto, Y. Tanaka, T. Furuhara, and T. Maki: *Acta Mater.*, 2006, vol. 54, pp. 4771–79.
27. G. Kurdjumov and G. Sachs: *Z. Phys.*, 1930, vol. 64, pp. 325–43.
28. S. Atamert and J.E. King: *Z. Metallkd.*, 1991, vol. 82, pp. 230–39.
29. C.Y. Chen, H.W. Yen, and J.R. Yang: *Scripta Mater.*, 2007, vol. 56, pp. 673–76.